

Multiple-port integrated optical circulators

Duanni Huang^{*1}, Paolo Pintus^{1,2}, Chong Zhang¹, Yuya Shoji³, Tetsuya Mizumoto³, John E. Bowers¹

⁽¹⁾ Dept. of Electrical and Computer Engineering, University of California, Santa Barbara, CA, USA,

⁽²⁾ Istituto TeCIP, Scuola Superiore Sant'Anna, Pisa, Italy,

⁽³⁾ Dept. of Electrical and Electronic Engineering / FIRST, Tokyo Institute of Technology, Tokyo, Japan

[*duanni@umail.ucsb.edu](mailto:duanni@umail.ucsb.edu)

Abstract— We present a path towards reconfigurable, electrically driven and integrated multiple-port optical circulators. Using this novel device architecture, we demonstrate a six-port circulator with 14.4 dB of isolation between adjacent ports, and four different working configurations. It can be straightforwardly expanded to larger port counts.

Keywords—Optical isolators, optical circulators, magneto-optic devices, Faraday rotation

I. INTRODUCTION

The circulator is a multiple-port device that routs light such that light entering any port exits from the next, much like a roundabout for photons. Many applications in data centers, telecommunications and sensors would benefit from bidirectional operation, which requires an optical circulator. Due to optical nonreciprocity, circulators often operate based on the magneto-optic Faraday effect. However, the transition from discrete to integrated optical circulators has been hindered by lattice and thermal mismatch between commonly used magneto-optic materials and silicon or III-V substrates.

Heterogeneous integration based on wafer bonding techniques has shown to be very promising as it circumvents the lattice mismatch problem [1-3]. Recently, we have demonstrated a high performance silicon-based integrated optical isolator with up to 32dB of isolation for transverse magnetic (TM) modes. The device was fabricated by bonding cerium substituted yttrium iron garnet (Ce:YIG) onto a silicon (Si) all pass ring filter [4]. Furthermore, our device architecture uses an integrated metallic microstrip to generate a current induced magnetic field for nonreciprocal behavior. This eliminates the need for permanent magnets, which are bulky and impede packaging. They also provide an efficient way to tune and switch magneto-optic devices. We have also shown optical circulators with dynamic reconfigurability using this design [5]. In this paper, we expand this design, showing that optical circulators with an arbitrary number of ports ($2N$) can be realized operating in one of many possible configurations (2^{N-1}). We then present experimental results from a six-port microring circulator as demonstration of this multiport architecture. To the best of our knowledge, this is the first integrated optical circulator with more than four ports.

II. DESIGN AND FABRICATION

The proposed device is shown in Fig. 1. It consists of two identical ring resonators and three bus waveguides fabricated using deep ultraviolet lithography on a 230nm thick silicon on insulator (SOI) wafer with a bonded 400nm Ce:YIG upper cladding. The waveguides are 600nm wide, so the largest

nonreciprocal phase shift can be achieved [6]. The two rings share a common bus waveguide, but are not coupled together. The ring radius is set to $20\mu\text{m}$ and the ring-waveguide gap is 200nm.

Following an O_2 plasma assisted direct bonding procedure, we thin the substrate of the bonded Ce:YIG die to roughly $10\mu\text{m}$, and then pattern a gold microstrip on top of each ring using a liftoff process. When we apply current through the two microstrips, they induce a radially outwards or inwards magnetic field with respect to the corresponding ring resonator. This causes a resonance wavelength split (RWS) in the ring between the clockwise (CW) and counterclockwise (CCW) propagating TM modes. Thus, light propagating between two ports will experience a different transfer function according to the direction.

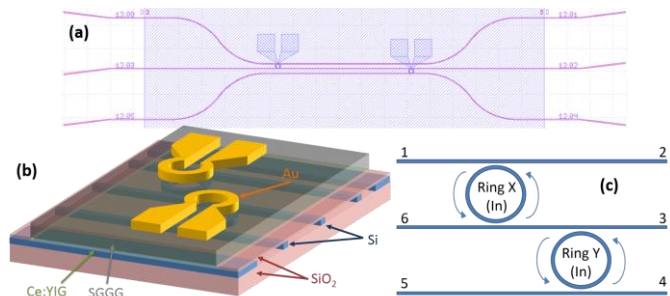


Figure 1: (a) Mask layout of the six-port circulator. (b) Schematic of the device. (c) One possible configuration of the circulator with the fields radially outward in both rings. The circulation direction is given by the arrows.

In the configuration shown in Fig 1c, the magnetic field is orientated outwards for both rings. When we align the operating wavelength to the CCW resonating mode, light going from the left to right will observe the ring out-of-resonance. Vice versa, for the light going from right to left, the rings are on-resonance and the light is dropped to the adjacent waveguide (i.e., port). As a result, the circulation among the ports is $1 \rightarrow 2 \rightarrow 3 \rightarrow 4 \rightarrow 5 \rightarrow 6 \rightarrow 1$. In this configuration, the proposed device can be seen as a cascade of two identical optical circulators presented in [1,5].

Furthermore, the magnetic field can be easily switched between inwards and outwards directions by reversing the current. Therefore, it is possible to dynamically reconfigure the circulation path. For the six-port circulator we have fabricated, we find that there are $2^2=4$ possible configurations, since each microstrip can be independently controlled. These are shown in Fig. 2. In general, the reconfigurable multi-port architecture presented here can be expanded to obtain arbitrary number of ports by adding additional rings and bus

waveguides in this manner. Using (N-1) rings with N bus waveguides can result in the realization of a 2N-port circulator with 2^{N-1} possible configurations. Circulators with an odd numbers of ports can be fabricated by adding a loop mirror at one port.

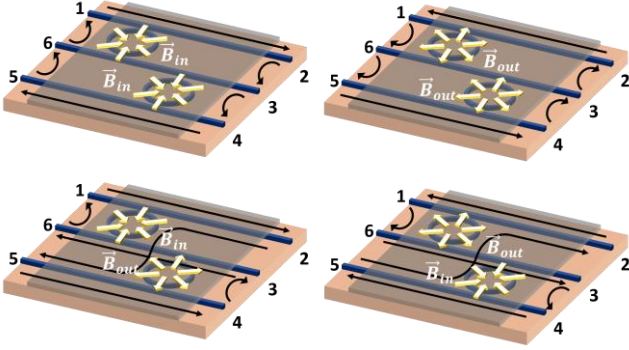


Figure 2: The four different configurations of the six-port circulator.

III. RESULTS

The six-port circulator is characterized by injecting TM polarized light into one of the ports using a tunable laser that is swept near 1550nm. Due to the angled facets, designed to reduce the reflections, we were unable to simultaneously measure the transmittance through all ports. Instead, we successively inject light from each port, and measure the spectra in the corresponding through and drop ports. The intrinsic spectra of the two rings are shown in Fig. 3a in which we measure the transmittance through the middle bus waveguide (Ports 3 and 6 in Fig. 2), capturing the resonance wavelength of both rings. Although the rings were designed to be identical, fabrication error and wafer nonuniformity causes over a 1nm difference between the two resonances. Therefore, we must also align the two rings in order for circulation at a common wavelength.

As we have previously shown, the microstrip can also serve as a thermal tuner for the ring [4]. We utilize this and apply different amounts of current to the two rings in order to align them in addition to generating the necessary magnetic field. We find the optimal conditions to be 185mA for the top ring and 262mA for the bottom ring. Under these conditions, the two resonances align, and there is sufficient magnetic field to establish a clear RWS between the CW and CCW modes. This is depicted in Fig. 3b for the top ring, and Fig. 3c for the bottom ring. Since the magnetic field strength is different for the two rings, the RWS is around 0.25nm for the top ring, and 0.35nm for the bottom ring. These measurements, along with others not pictured here, allow us to complete the scattering matrix S, which relates the input signal at port j (i.e., A_j^+) to the output signal at port i (i.e., $A_i^- = \sum S_{ij} A_j^+$).

$$20 \cdot \log_{10} [abs(S)] = \begin{bmatrix} - & -11.5 & - & - & - & -12.6 \\ -22.5 & - & -12.1 & - & -23.0 & - \\ - & -26.5 & - & -11.3 & - & -30.3 \\ - & - & -15.5 & - & -12.0 & - \\ - & -20.4 & - & -23.5 & - & -14.3 \\ -10.1 & - & -29.3 & - & -27 & - \end{bmatrix}$$

Here, the highlighted entries of the scattering matrix show the proper circulation path, and the largest isolation, or difference between S_{ij} and S_{ji} , is measured between two adjacent port (i.e., port 2 and port 3) is 14.4 dB. This can be improved if the two rings were nearly identical so that a RWS of 0.35nm was obtained for both rings. All powers have been normalized to a silicon reference waveguide without the garnet cladding. Design improvements such as a multi-coil microstrip similar to magnetic recording heads can also increase the RWS and thus the performance of the circulator.

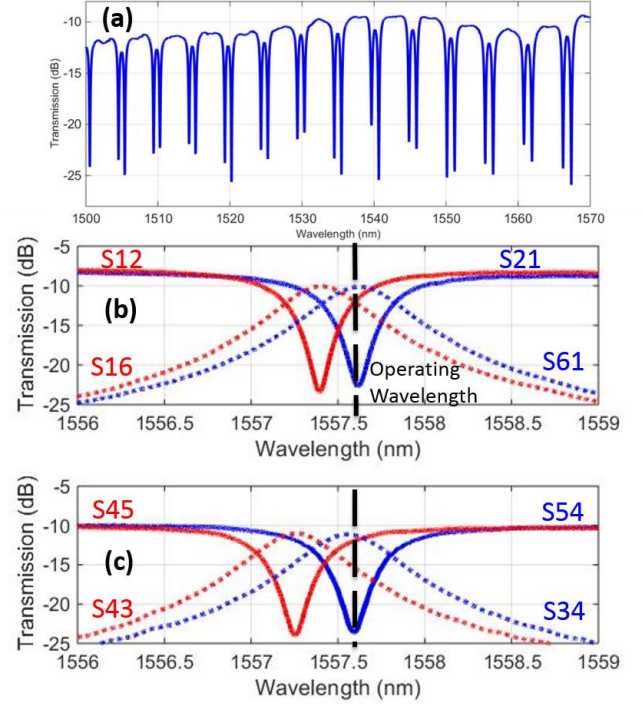


Figure 3: (a) Intrinsic spectrum of the two rings with no magnetic field. The transmission through the top ring (b) and the bottom ring (c) are shown, with clear evidence of RWS and optical nonreciprocity.

IV. CONCLUSIONS

We experimentally demonstrated an integrated silicon-based six-port circulator with 14.4dB of isolation between adjacent ports. The proposed device can be dynamically reconfigured and expanded to even larger number of ports. It can be effectively used in integrated optics and could lead to novel reconfigurable optical networks and switching elements.

REFERENCES

- [1] P. Pintus, et al. "Integrated TE and TM optical circulators on ultra-low-loss silicon nitride platform," *Opt. Express* **21**(4) 5041-5052 (2013).
- [2] Y. Shoji, et al. "Magneto-optical isolator with silicon waveguides fabricated by direct bonding," *Appl. Phys. Lett.* **92**, 071117 (2008).
- [3] M.-C. Tien, et al. "Silicon ring isolators with bonded nonreciprocal magneto-optic garnets," *Opt. Express* **19**, 11740-11745 (2011).
- [4] D. Huang, et al. "Silicon microring isolator with large optical isolation and low loss" *Optical Fiber Communications Conference* (2016).
- [5] D. Huang, et al. "Reconfigurable integrated optical circulator" *CLEO* (2016).
- [6] P. Pintus, et al. "Design of magneto-optical ring isolator on SOI based on the finite-element method," *IEEE Photon. Technol. Lett.*, **23**, 1670-1672 (2011).